Spin and Polarized Current from Coulomb Blockaded Quantum Dots

R. M. Potok,[1] J. A. Folk,[1,2] C. M. Marcus,[1] V. Umansky,[3] M. Hanson,[4] and A. C. Gossard[4]

[1]*Department of Physics, Harvard University, Cambridge, Massachusetts 02138, USA*
[2]*Department of Physics, Stanford University, Stanford, California 94305, USA*
[3]*Braun Center for Submicron Research, Weizmann Institute of Science, Rehovot, 76100, Israel*
[4]*Materials Department, University of California, Santa Barbara, Santa Barbara, California 93106, USA*
(Received 2 March 2003; published 3 July 2003)

We report measurements of spin transitions for GaAs quantum dots in the Coulomb blockade regime and compare ground and excited state transport spectroscopy to direct measurements of the spin polarization of emitted current. Transport spectroscopy reveals both spin-increasing and spin-decreasing transitions, as well as higher-spin ground states, and allows g factors to be measured down to a single electron. The spin of emitted current in the Coulomb blockade regime, measured using spin-sensitive electron focusing, is found to be polarized along the direction of the applied magnetic field regardless of the ground state spin transition.

Quantum dots in the Coulomb blockade (CB) regime have for several years provided a valuable tool to study spin in confined systems. Systems with small interactions, such as nanotubes [1] and nonmagnetic metal grains [2], show signatures of spin degenerate orbital levels with electrons filling in a simple Pauli scheme of spin $0, \frac{1}{2}, 0, \frac{1}{2}, \ldots$. In contrast, recent transport measurements in lateral GaAs quantum dots [3–5] suggest the existence of higher-spin ground states.

In this Letter, we explore ground and excited spin states of few- and many-electron lateral GaAs dots in the weak tunneling regime, using both transport spectroscopy as well as a focusing measurement that allows a direct determination of the spin polarization of emitted current [6]. Consistent with previous work [3–5] we find, as evidence of higher-spin ground states in the larger dot, that spin transitions (increasing or decreasing) are often followed by a second transition in the same direction as electrons are added to the dot. Excited state spin transitions and spin degeneracy for several quantum levels are also explored using nonlinear bias spectroscopy, and clear spin splitting is found for the $N = 1$ electron case in the few-electron dot. It is generally believed [7] that opposite state spin transitions lead to opposite spin polarizations of the emitted current on Coulomb blockade peaks. We find instead that the spin polarization of the current is the same for CB peaks corresponding to spin-increasing and spin-decreasing transitions, with the polarization always aligned with the external magnetic field.

Measurements were performed on two quantum dots, one with many electrons ($N \sim 100$) and the other with few electrons ($N < 10$). In the small dot we concentrate on the $N = 0 \rightarrow 1$ electron transition. Focusing measurements of spin polarization of emitted current were performed for the larger quantum dot. The devices were fabricated using Cr/Au depletion gates on the surface of a GaAs/Al$_x$Ga$_{1-x}$As heterostructure; the two dimen-

sional electron gas (2DEG) was contacted using nonmagnetic PtAuGe Ohmics. For the larger dot [Fig. 1(a)], $x = 0.36$, the 2DEG was 102 nm from the surface, density was $n = 1.3 \times 10^{11}$ cm^{-2}, dot level spacing was $\Delta \sim 70 \ \mu$eV, and charging energy was $E_c \sim 800 \ \mu$eV. The high mobility of this 2DEG, $\mu = 5.5 \times 10^6$ cm^2/V s, allowed the observation of several clear focusing peaks. The smaller quantum dot [Fig. 2(b), inset [8]] was fabricated on a different heterostructure ($x = 0.3$) with density 2.3×10^{11} cm^{-2} and mobility 5×10^5 cm^2/V s.

Experiments were carried out in a dilution refrigerator with base electron temperature $T_e = 70$ mK (determined by CB peak width), using standard ac lock-in techniques with an excitation voltage of 5 μV. A pair of tranverse superconducting magnets was used to provide independent control of field in the plane of ($B_\parallel$) and perpendicular to ($B_\perp$) the 2DEG [9].

On a CB peak, transport through an N-electron dot occurs via the addition and removal of the $N + 1$ electron, with the corresponding z component of the dot spin, $S_z(N)$, changing to $S_z(N + 1)$ and back again. The energy required for this transition as measured by CB peak position depends on the the magnetic field B through a Zeeman term, $-g\mu B[S_z(N + 1) - S_z(N)] = -g\mu B(\Delta S_z)$. The spacing between $N \rightarrow N + 1$ and $N + 1 \rightarrow N + 2$ CB peaks is given by $-g\mu B\{[S_z(N + 2) - S_z(N + 1)] - [S_z(N + 1) - S_z(N)]\}$. (Orbital magnetic coupling is minimized by applying a purely in-plane field, $B_\parallel$.) A CB peak position that moves upward (downward) in gate voltage [upward (downward) in the energy required to add an additional electron] as a function of field indicates a spin-decreasing (spin-increasing) transition. A spin-increasing transition of ΔS_z followed by an spin-decreasing transition of $-\Delta S_z$ yields a peak spacing that increases with field; for the opposite sequence, the peak spacing decreases with field. For the case of $\Delta S_z = \frac{1}{2}$ transitions, the slopes of the spacings will be $\pm g\mu$. Consecutive transitions of the same magnitude and in
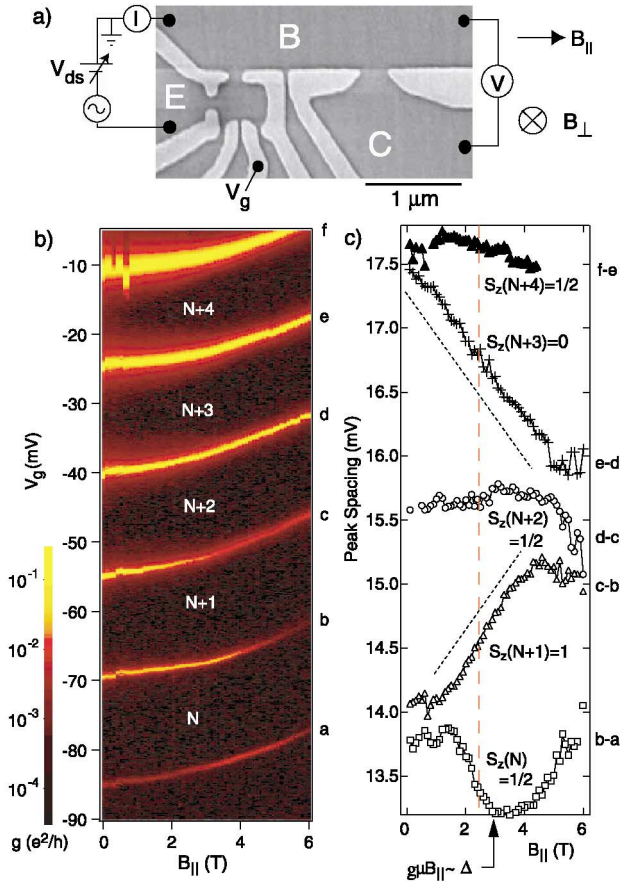
FIG. 1 (color). (a) Micrograph of a quantum dot, similar to the one measured, in a focusing geometry. A voltage is applied from emitter (E) to base (B) regions; emitter current and base-collector (B-C) voltage give dot conductance and focusing signal, respectively. (b) Six consecutive Coulomb blockade peaks in the weak tunneling regime (valley conductance near zero), measured as a function of gate voltage, V_g, and in-plane magnetic field, $B_\parallel$. A Hall bar fabricated on the same chip allows the perpendicular field, $B_\perp$, to be measured simultaneously and held at ~ -110 mT. (c) Peak spacings (in V_g) extracted from the data in (b). From the slopes of these lines in $B_\parallel$, the spin transition associated with each Coulomb blockade peak may be determined. For example, at $B_\parallel = 2.5$ T (red dashed line) a possible sequence of ground spin states resulting from these transitions is shown. The dotted black lines indicate expected slopes of peak spacing for $S_z(N) \rightarrow S_z(N) \pm \frac{1}{2}$ transitions, using $g = 0.44$. Spacings offset for clarity.

the same direction, for instance $S_z = 0 \rightarrow \frac{1}{2} \rightarrow 1$, yield a peak spacing that does not change with field.

Six consecutive CB peaks as a function of magnetic field for the larger dot are shown in Fig. 1(b). The parabolic dependence of peak position on $B_\parallel$ is believed to result from the effect of the field on the well confinement potential [3,10]; this effect gives the same shift for all CB peaks and so disappears when the peak spacing is extracted. Corresponding CB spacings, shown in Fig. 1(c), display linear motion with slopes $\pm g\mu$ and zero, where

the g factor is consistent with the bulk value for GaAs, $g = -0.44$.

Beginning from an arbitrary value of spin for the N electron dot, $S_z(N)$, we can enumerate the ground state spin transitions for the dot as additional electrons are added (peak spacing only spin transitions, not magnitudes). For example, in Fig. 1(c) at 2.5 T, the spacing for the two peaks at the most negative gate voltage (fewest electrons) decreases with $B_\parallel$, suggesting that $S_z(N + 1) = S_z(N) + \frac{1}{2}$ and $S_z(N) = S_z(N - 1) - \frac{1}{2}$. Taking $S_z(N) = \frac{1}{2}$ gives a spin structure for the states shown in Fig. 1 (labeled $N - 1, N, \ldots, N + 5$) of $(1, \frac{1}{2}, 1, \frac{1}{2}, 0, \frac{1}{2}, 1)$ at $B = 2.5$ T. The occurrence of peak spacings with zero slope is evidence of higher-spin ground states. We note that no two consecutive spacings both have slopes $+g\mu$ or $-g\mu$, which would indicate pin changes of $\frac{3}{2}$ or greater upon adding an electron. (Because of the negative g factor in GaAs, the lower-energy spin state for a single electron will generally be antialigned with an external magnetic field; therefore, we define $S_z = +\frac{1}{2}$ to be antialigned with the field; one may then use a positive g factor for energy calculations.)

Excited state spin transitions can be observed using finite dc drain-source bias, $V_{ds} > g\mu B$. A change in spin between two states (either ground or excited) of the N and $N + 1$ electron systems would be expected to cause the corresponding peak in differential conductance to shift with B [1,2]. Furthermore, any transition which is spin degenerate at $B = 0$ should split as a function of field. Excited state transitions from several consecutive Coulomb blockade peaks in the larger dot are shown at $V_{ds} = 400$ μV as a function of B and V_g in Fig. 2(a). Splitting of excited state features with field is only occasionally observed, suggesting a lack of spin degeneracy for many of these transitions. At the same time, some distinct transitions move toward or away from each other with slopes $\pm g\mu$, possibly indicating differences in dot spin for initial and final states.

We also measured spin transitions for the $N = 0 \rightarrow 1$ electron transition using the smaller dot [Fig. 2(b), inset]. Finite drain-source measurements were used to find the $0 \rightarrow 1$ electron transition; see Fig. 2(b) [11]. This transition displays clear splittings for both the ground and first excited states [Fig. 2(c)], with g factors measured to be $g \sim 0.37$. When more electrons were added to the device (for example, for the $1 \rightarrow 2$ electron transition or even more clearly for $2 \rightarrow 3$ or higher transitions) splittings were only occasionally observed (data not shown). The simpler behavior for the $0 \rightarrow 1$ electron transition may indicate the important effect of interactions on the spin structure of multielectron dots [12].

In the absence of spin blockade [10,13], one would expect S_z of the dot to change by the the spin $s_z = \pm \frac{1}{2}$ of the electron added to it: $S_z(N + 1) = S_z(N) + s_z$. This would imply opposite polarization of transport current for spin-increasing and spin-decreasing transitions [7].
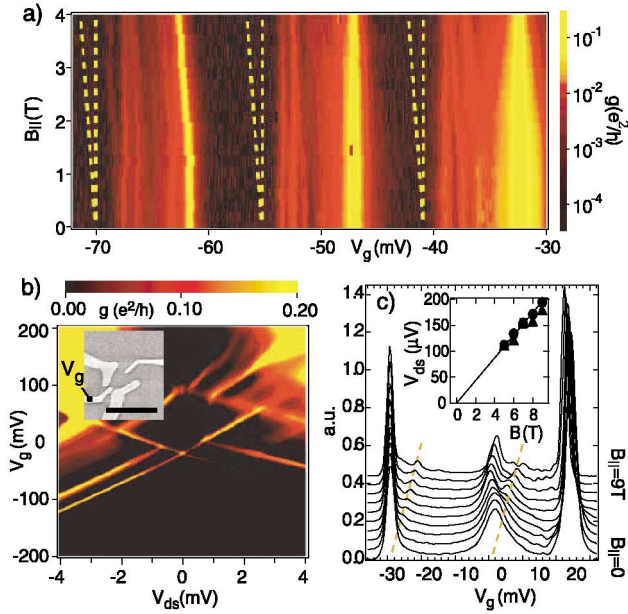
FIG. 2 (color).   (a) Color plot of the differential conductance of Coulomb blockade peaks at $V_{ds} = 400\ \mu$V, as a function of V_g and $B_\parallel$ ($B_\perp$ held constant at -110 mT) for the quantum dot shown in Fig. 1. (All V_g traces were shifted to align the rightmost peak.) For comparison the dashed lines show an energy separation of $g\mu B$, taking $g = 0.44$. Splitting is only occasionally observed. (b),(c) Similar measurements taken on a different quantum dot [micrograph shown in (b) inset, scale bar is 1 μm]. (b) Coulomb diamond at $B_\parallel = 0$ and $B_\perp = -200$ mT demonstrating that the CB peak near $V_g = 0$ is the $0 \to 1$ electron transition. (c) Differential conductance of the $0 \to 1$ electron CB peak at $V_{ds} = 1200\ \mu$V from $B_\parallel = 0$ to 9 T (curves offset for clarity, and individually rescaled to have a constant height for the rightmost peak). In contrast to (a), clear spin splitting of ground and excited states is seen for this transition (dashed yellow lines are guides to the eye). Inset: splitting as a function of B for the ground state (solid circles) and first excited state (solid triangles). Solid line shows best fit to the data and gives a g factor of 0.37.

We examine this expectation experimentally by comparing the spin transitions determined by CB peak position to a direct measurement of the spin polarization of current emitted on a CB peak.

The spin polarization of current from the quantum dot was measured in a transverse focusing geometry [Fig. 1(a)]. As described previously [6,14], the height of a focusing peak reflects the degree (and direction) of spin polarization of current from the emitter when the collector quantum point contact (QPC) is spin selective, according to the relation $V_c = \alpha I_e (h/2e^2)(1 + P_e P_c)$. Here V_c is the focusing peak height, I_e is the total emitter current with polarization $P_e = (I_{\uparrow e} - I_{\downarrow e})/(I_{\uparrow e} + I_{\downarrow e})$, and $P_c = (T_{\uparrow c} - T_{\downarrow c})/(T_{\uparrow c} + T_{\downarrow c})$ is the spin selectivity of the collector. [The efficiency parameter α $(0 < \alpha < 1)$ accounts for spin-independent imperfections in the focusing process.]

Using a Coulomb blockaded quantum dot as the emitter favors the use of a voltage bias between emitter and base, rather than a current bias as used in Refs. [6,14]. In this case, changes in the emitter current, I_e, lead to changes in the focusing peak height even when its polarization remains constant. To study spin polarization, we measure the emitter current along with the collector voltage [Figs. 3(a) and 3(b)] and use the quantity V_c/I_e, a *nonlocal* resistance, as a measure of the spin polarization of the current from the CB quantum dot when the collector is spin selective. For a spin-selective collector ($g_c = 0.5e^2/h$, in an in-plane field), the value of V_c/I_e should range from twice the value found in the unpolarized case ($g_c = 2e^2/h$), when emitter polarization and collector selectivity are oriented in the same direction, to zero, when the spin directions are oppositely oriented.

Simultaneous focusing and conductance measurements at $B_\parallel = 6T$ for both spin-selective and spin-independent collector are presented in Figs. 4(a) and 4(b), as the dot is tuned from the semiopen to the weak tunneling regimes using the voltage, V_g, on the side gate. We find that the focusing signal V_c/I_e with spin-selective collector ($g_c = 0.5e^2/h$) always lies above the signal with
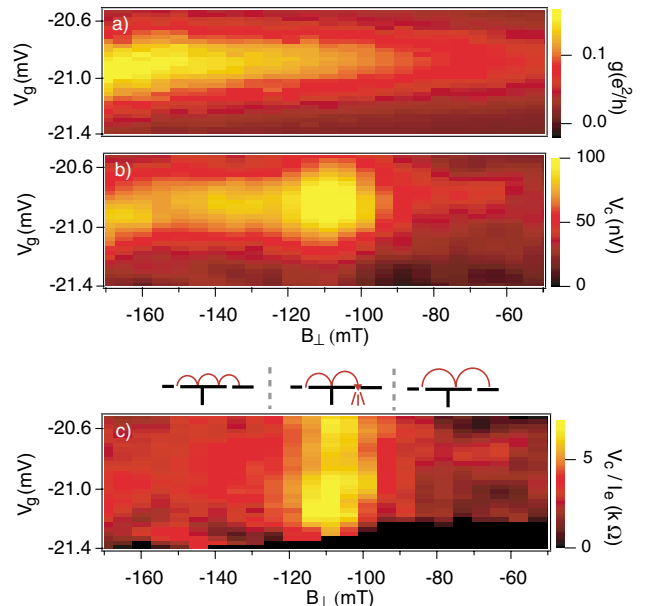

FIG. 3 (color).   (a) Conductance of a CB peak as a function of both V_g and $B_\perp$, for the dot shown in Fig. 1(a) in a focusing geometry. (b) B-C voltage, V_c, measured at the same time as the dot conductance, near $B_\perp = -110$, corresponding to the second focusing peak (the second peak was used because it was affected least by $B_\parallel$ in this device). (c) The nonlocal resistance V_c/I_e most clearly shows the effect of focusing. The diagrams indicate the electron focusing condition for fields near the second focusing peak. The location of the focusing peak in $B_\perp$ remained constant for all CB peaks studied. Data do not appear when $g_e < 0.1e^2/h$ ($I_e < 20$ pA, $V_c \lesssim 40$ nV) because the ratio V_c/I_e becomes unreliable.
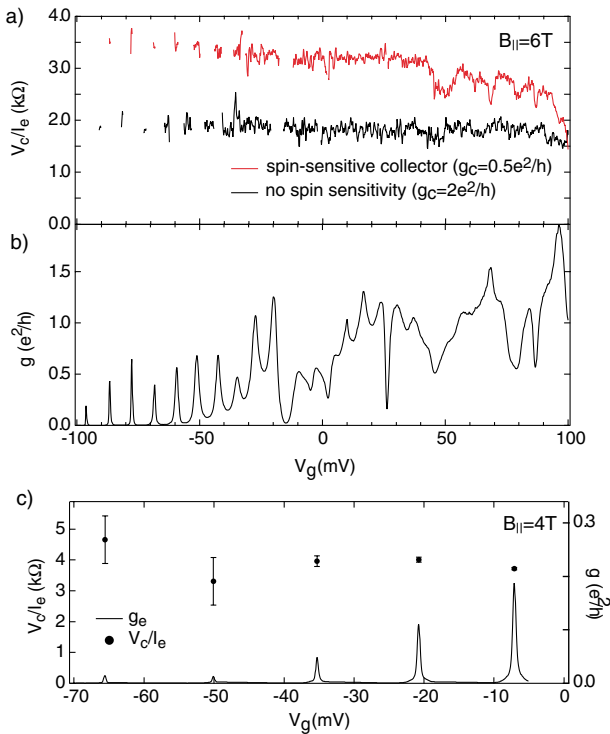
FIG. 4 (color). (a) Focusing signal at $B_\| = 6$ T from the quantum dot shown in Fig. 1, with spin-selective ($g_c = 0.5e^2/h$, red curve) and spin-independent ($g_c = 2e^2/h$, black curve) collectors. The polarization of current fluctuates on a typical gate voltage scale of $V_g = 5$ mV, but these fluctuations are suppressed as V_g is reduced below 30 mV. At the same time, the spin selective curve rises to nearly twice the value as the curve at $g_c = 2e^2/h$, indicating spin polarization of the emitter current (see text). (b) Conductance measured simultaneously with data in (a). (c) Focusing signal and conductance measured for the CB peaks shown in Fig. 1 ($N + 1$ to $N + 6$) at $B_\| = 4$ T and $g_c = 0.5e^2/h$. Again, only small fluctuations in the focusing signal are observed despite different spin transitions observed for these peaks in Fig. 1. Based on the increase of V_c/I_e to 3.5 from 1.9 kΩ with the spin selective collector in (a), we would have expected the focusing peak to be suppressed to $V_c/I_e \sim 0.3$ kΩ if the opposite polarization were generated at the emitter. (Collector selectivity depends only weakly on B at these fields and temperatures [6].)

spin-independent collector ($g_c = 2e^2/h$) once the dot is tuned into the weak tunneling regime. This suggests that the current emitted from the quantum dot at low conductance is always spin polarized in the same direction as the collector, over a range of gate voltage where many electrons are added.

Figure 4(c) shows focusing measurements for the same peaks shown Fig. 1, at $B_\| = 4$ T. Spin transitions of both directions were observed based on peak motion (see Fig. 1), whereas spin polarization of emitted current is

again found to remain nearly constant over all measured CB peaks. This observation is inconsistent with the picture of spin transitions leading to $S_z(N + 1) = S_z(N) + s_z$ discussed earlier.

We note as well that there is no apparent correlation between peak height and spin transition in a large in-plane field. It was shown in Refs. [6,14] that the leads of a quantum dot become spin polarized in the same way as single QPC's in an in-plane field. However, a spin dependent tunnel barrier should lead to a dramatic suppression in CB peak height for spin-decreasing transitions. As seen in Fig. 1, this was not observed in our measurement. Taken together, these observations may indicate that spin polarization in the leads is playing a role in the spin state of the quantum dot on a CB peak.

In conclusion, we have found signatures of spin-increasing and spin-decreasing transitions in transport, including spin splitting of the $N = 0 \rightarrow 1$ transition. Measured polarization of the current emitted from a quantum dot in the CB regime is in all cases polarized in the same direction as the QPC collector, for both spin-increasing and spin-decreasing transitions of the dot. These observations necessitate a revised picture of spin transitions in a lateral quantum dot in an in-plane magnetic field.

[1] D. H. Cobden *et al.*, Phys. Rev. Lett. **81**, 681 (1998).
[2] D. C. Ralph, C. T. Black, and M. Tinkham, Phys. Rev. Lett. **78**, 4087 (1997).
[3] D. S. Duncan *et al.*, Appl. Phys. Lett. **77**, 2183 (2000).
[4] J. A. Folk *et al.*, Phys. Scr. **T90**, 26 (2001).
[5] S. Lindemann *et al.*, Phys. Rev. B **66**, 195314 (2002).
[6] R. M. Potok, J. A. Folk, C. M. Marcus, and V. Umansky, Phys. Rev. Lett. **89**, 266602 (2002).
[7] P. Recher, E. V. Sukhorukov, and D. Loss, Phys. Rev. Lett. **85**, 1962 (2000).
[8] M. Ciorga *et al.*, Phys. Rev. B **61**, 16315 (2000).
[9] J. A. Folk *et al.*, Phys. Rev. Lett. **86**, 2102 (2001).
[10] J. Weis, R. J. Haug, K. V. Klitzing, and K. Ploog, Phys. Rev. Lett. **71**, 4019 (1993).
[11] L. P. Kouwenhoven *et al.*, Science **278**, 1788 (1997).
[12] X. Hu and S. Das Sarma, condmat/0102019.
[13] D. Weinmann, W. Hausler, and B. Kramer, Phys. Rev. Lett. **74**, 984 (1995).
[14] J. A. Folk, R. M. Potok, C. M. Marcus, and V. Umansky, Science **299**, 679 (2003).